ULSI Quality Silicon Epitaxial Growth at 850°C

V. J. Silvestri,* K. Nummy, P. Ronsheim, R. Bendernagel, D. Kerr,* and V. T. Phan

IBM General Technology Division, Hopewell Junction, New York 12533

J. O. Borland* and J. Hann

Applied Materials, Incorporated, Santa Clara, California 95054

ABSTRACT

ULSI quality silicon epitaxial films as thin as 0.6 μm have been grown using dichlorosilane at temperatures as low as 850°C and pressures as low as 10 torr in commercially available cylindrical epi reactors. Removal of the substrate surface native oxide by a 5 min hydrogen bake has been observed down to 850°C, 10 torr. In addition, very low defect levels and excellent device characteristics have been measured in the epitaxial films. The results were observed on both 125 and 200 mm substrates.

ULSI processes for Si epitaxy must minimize dopant movement and autodoping effects. Films with carrier concentration changes of up to four orders of magnitude over transition widths of less than 0.2 μm are needed. For some applications these films must be thin (0.5 μm) and virtually defect-free. In conventional VLSI epitaxy processes, prolonged high-temperature hydrogen bakes and HCl etches are used before epitaxial growth to remove the surface native oxide and to strip the near-surface contaminants which initiate defects in the epitaxial films. These lengthy high-temperature hydrogen treatments are intolerable if autodoping and diffusion are to be minimized. As exercised in conventional epitaxial reactors, these pre-epitaxial treatments are necessary to eliminate the native oxide and additional oxide grown by oxidizers present in the system and reactant gases.

Historically, moderate success has been achieved in controlling autodoping by employing an extended high-temperature (1150°C) prebake in hydrogen. This serves to outgas the dopants from the surface prior to subsequent film growth at 1050°C. This has been called the "Hi-Lo" process and was developed by Srinivasan (1). Later it was shown that abrupt doping profiles could be achieved on heavily doped substrates by employing a two-step deposition which included growth of an undoped silicon film followed by a more lightly doped silicon film (2). Although the original interface of the highly doped region diffuses into this undoped layer, semi-abrupt junctions were achieved in submicron films grown at atmospheric pressure. The present work has examined autodoping profiles using a similar two-step process for a lower temperature range at reduced pressure.

The development of lower pressure (50-200 torr) epitaxial systems has resulted in lower background levels of oxidizers which allows the use of lower temperatures for film growth with less intensive pre-epitaxial heat-treatments. The development of ultra-low pressure (ULP, 0.001 torr) systems has allowed excellent films to be grown at temperatures between 570°-800°C (3, 4). This success has highlighted the need for cleaner epi systems designed to operate in the medium temperature range (850°-1000°C). The ULP systems virtually eliminate autodoping and diffusion and can provide very abrupt dopant transitions due to the low temperatures employed. The ULP systems, however, have been limited to low deposition rates (5-100 Å/min) which are not practical for thick (>0.5 μm) film growth. The need for abrupt dopant profiles still exists for these thick films. A new focus on conventional epi systems has therefore been to emulate the features of ULP tools (*i.e.*, a lower base pressure allowing growth at lower temperatures) without losing growth rates practical for thicker films.

The emphasis in this work has been to explore the medium temperature growth range using deposition pressures in the 10-30 torr pressure range. The medium temperature epi (MTE) films were grown in an AMC 7810 reactor and were later demonstrated in a Precision 7700 Epi system as well. The experiments have examined various temperature bakes and their effectiveness in removing the native oxide prior to MTE deposition. The oxygen and carbon content at the interface was observed using SIMS analysis following film growth. These observations were correlated with measurements of the film quality. Dopant concentration profiles were examined using both spreading resistance and SIMS analysis. Vertical profiles were characterized on n+ and p+ silicon. Lateral and vertical autodoping effects were studied in films where both heavily doped n+ and p+ ion implanted regions were present on the initial surface.

The reduction of the amount of oxide present at the silicon epitaxial interface has enabled us to grow films with abrupt vertical profiles at temperatures as low as 850°C at 10 torr. This work has shown that conventional reduced pressure epitaxial reactors can provide high quality silicon films in the medium temperature range and can achieve deposition rates appropriate for thick films.

Experimental

Dichlorosilane, hydrogen, and arsine gases were used in depositing the films. A pressure range of 10-30 torr was employed. Films were grown both with and without prebake treatments in the thickness range of 0.6-3.3 μm. Carrier concentration profile measurements were made using SIMS and spreading resistance techniques. Characterization techniques addressing film quality included Yang (5) and Wright (6) etching, TEM, and pulsed MOS measurements (7). Evaluations of oxide removal at surfaces used SIMS, although visual and microscopic characteristics in the form of haze on the deposited films were good indicators of underlying oxide. Presence of carbon at the surfaces was examined as well.

In separate experiments the two-step epitaxial growth sequence was employed in which a 0.5 min undoped silicon cap was grown (750-1000Å) followed by deposition of the doped silicon layer. No prebake of the substrate was used for the "cap" process. The lightly doped n-type films were grown on blanket heavily doped n and p silicon. Similarly n-type silicon was deposited over surfaces having both n- and p-type regions exposed on the same wafer. Lateral autodoping was assessed for the latter films and will be discussed below.

Results and Discussion

Thickness and resistivity uniformities.—For these experiments thickness and resistivity uniformities were evaluated in the AMC 7810 and a Precision 7700 Epi radiant heating epitaxial reactor. Tests were run at 860°C and 35 torr for 200 mm wafers. Results on the AMC 7810 for thickness uniformities at 3 μm were ±2.9% and resistivity at 0.6 Ω-cm were ±9.0%. On the Precision 7700 Epi, thickness uniformities were ±3.5% and resistivity uniformities ±6.5%. The load size on the AMC 7810 was 4-200 mm wafers with a three-zone temperature control while on the Precision 7700 Epi, 8-200 mm wafers were loaded with a

* Electrochemical Society Active Member.

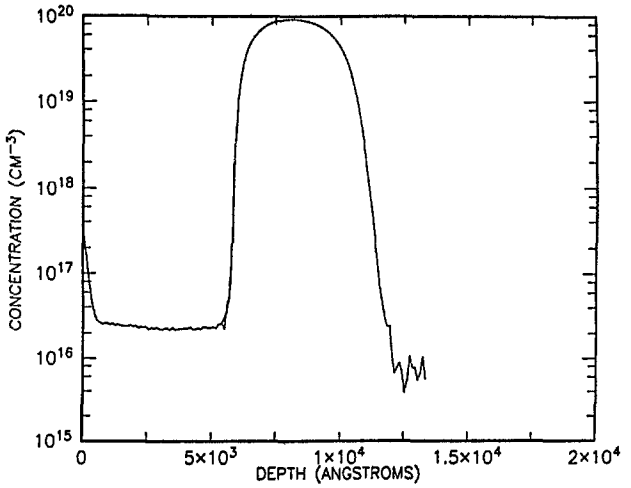

Fig. 1. SIMS dopant profile for a 0.6 μm n-epitaxial film on an n+ substrate.

nine-zone temperature control. The deposition rates for the MTE experiments in this study were in the range of 570-2000 Å/min.

Dopant profiles.—Figures 1-4 show typical SIMS profiles obtained for several MTE growth conditions. Figure 1 shows the vertical SIMS profile for an arsenic-doped film over a heavily doped n+ ion implanted surface. The film was deposited at 860°C and the data show a 3.5 order of magnitude dopant concentration change in less than 0.2 μm of film growth. Figure 2 shows a typical curve for a 0.9 μm film on an n+ surface where oxygen was measured at the interface. Both oxygen and carbon could be observed at the growth interface under certain conditions of growth which will be discussed in later figures. Figures 3 and 4 show vertical profiles for n-type films deposited over n+ arsenic and p+ boron doped blanket ion implanted silicon substrates. These films were deposited employing the two-step epitaxial growth sequence described above. The films were deposited at 860°C following the 0.5 μm undoped cap growth. It should be noted that no peak is observed at the interface for the oxygen curves for the growth conditions in Fig. 3 and 4. Instead the oxygen level is seen to lie below 1×10^{18} atom/cm^3 the normal background observed for float zone silicon. The capping process was effective in reducing autodoping for these blanket implanted films similar to the use of low temperature growth for the film in Fig. 1.

Vertical and lateral autodoping.—The steep dopant profiles obtained in Fig. 1, 3, and 4 show that vertical autodoping can be mitigated by employing low bake and growth

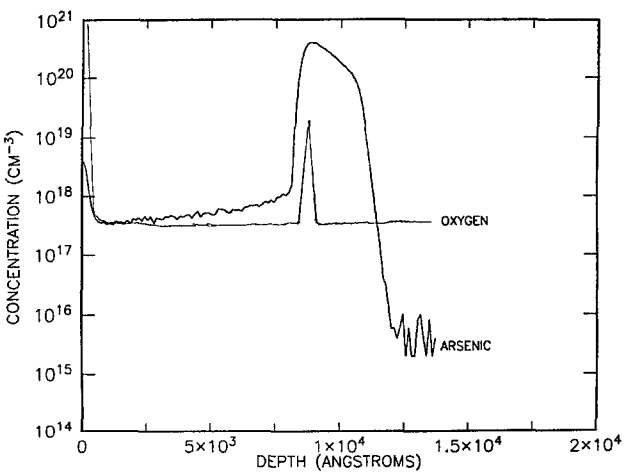

Fig. 2. SIMS dopant profile for a 0.9 μm film showing oxygen peak at growth interface.

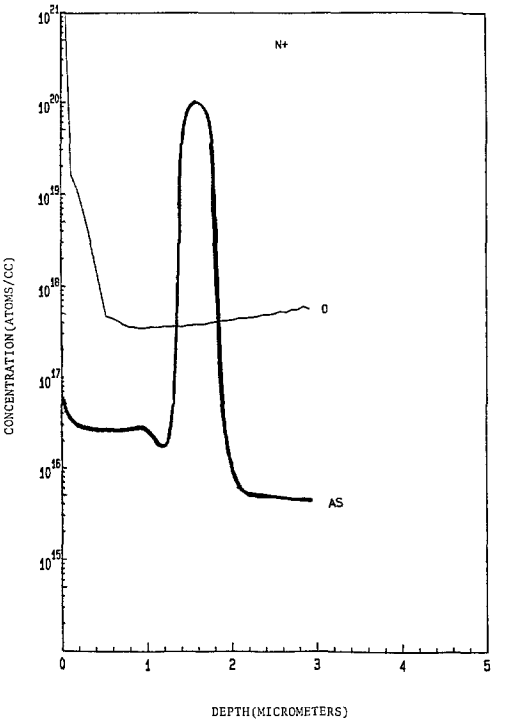

Fig. 3. SIMS dopant profile for an n-type epitaxial film deposited on an n+ /// surface using cap/deposit process.

temperatures as well as by using a cap layer process. For Fig. 1 the hydrogen bake was carried out at 1000°C preceding the growth at 860°C for 20 min. For the capped deposition in Fig. 3 and 4 the cap layer was deposited at 1150°C for 0.5 min. This step functions to anneal and outgas the dopant nearest the surface. In addition, the high deposition rate at this temperature caps the surface quickly to prevent the further release of dopant into the gas-phase which increases autodoping in the films. Both spreading resistance and SIMS were used to examine profiles and the spreading resistance data tracked qualitatively the SIMS profiles.

Lateral autodoping was also evaluated for film growth on silicon having both n+ and p+ regions exposed. For

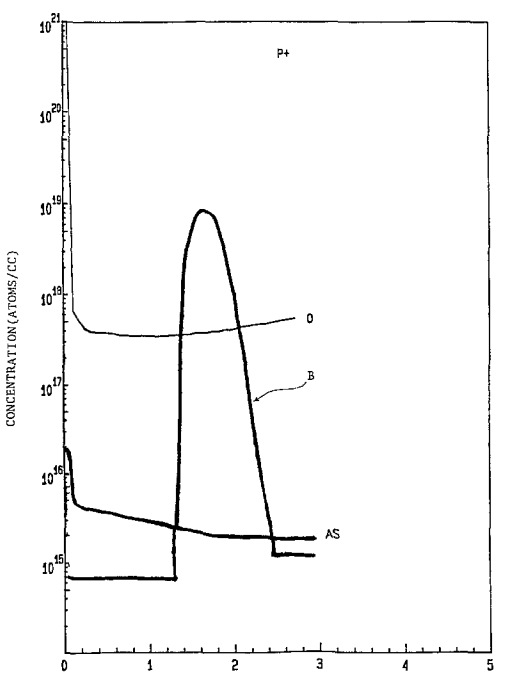

Fig. 4. SIMS dopant profile for an n-type epitaxial film deposited on a p+ /// surface using cap/deposit process.

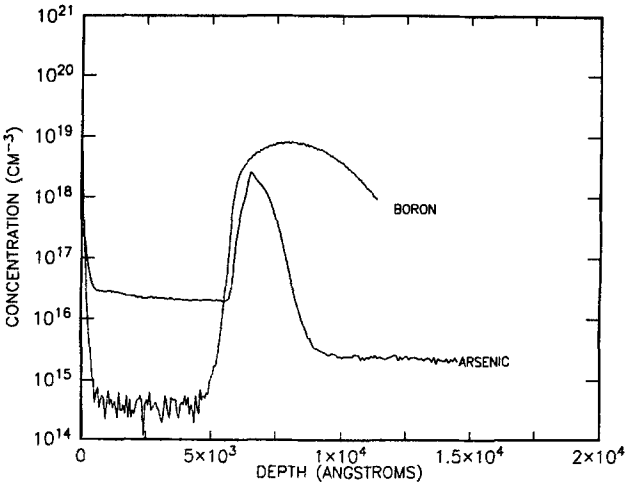

Fig. 5. SIMS dopant profile showing lateral autodoping of arsenic in an n-type epitaxial film over p+ /// surface.

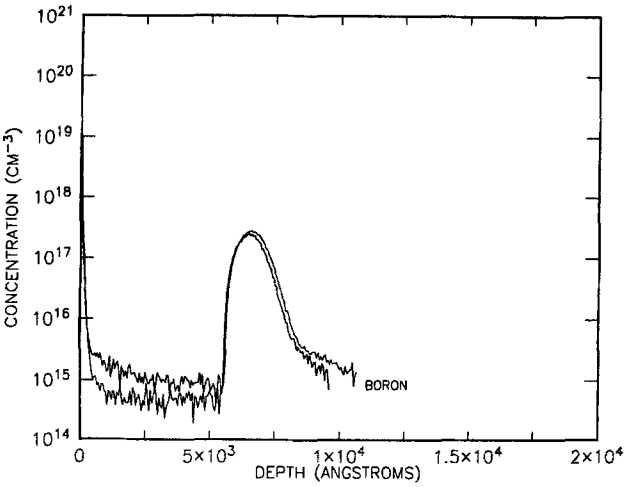

Fig. 7. SIMS profiles showing boron concentrations at 30 and 600 μm from a p+ region.

these experiments the two-step process was employed with 0.5 min cap followed by deposition of lightly doped n-type silicon at 860°C. The run pressure for this experiment was 32 torr. SIMS analysis was used to measure arsenic concentration in the epitaxial film over the heavily doped boron regions and boron concentration in the epitaxial film deposited over the heavily doped arsenic regions. The data appear below in Fig. 5 and 6. The data in Fig. 5 were taken centrally through the epi film over a p+ square 400 μm in width. The data show a pronounced arsenic peak of approximately 1×10^{18} atom/cm^3 near the expected growth interface of the deposited film of 0.6 μm thickness. This peak shows the significant outgassing which takes place in the initial growth stage at the interface when mixed surfaces are present. The boron autodoping is shown in Fig. 6 and occurs to a much lesser degree 2×10^{17} atom/cm^3 for the experimental conditions. Figures 7 and 8 track the lateral migration and incorporation in the epi film. The data show that concentrations of both arsenic and boron are essentially the same over significant distances. For example, the two curves for boron were taken from data collected at 30 and 600 μm from a p+ buried region edge. Likewise, for arsenic similar concentrations were found in the epi film over the p+ regions at 30 and 200 μm from an arsenic edge.

Oxide removal (in situ hydrogen bake).—Oxide present at the interface of the epitaxial film was examined for a number of bake and growth conditions in the temperature range of 850°-1000°C at 10 torr pressure. The SIMS data is shown in Fig. 9B, C, and D and Fig. 10A and B. In Fig. 9A, data for oxygen level in float zone n-type silicon taken with the experimental samples are shown for comparison. The bake temperatures shown in the figures were for a similar time of 5 min and growth times for deposition conditions shown in figures were all kept at 20 min for the films. In Fig. 9B and C for hydrogen bakes of 1000° and 950°C, oxygen levels are the same as those found in float zone substrates. The same low oxygen concentrations were observed for films deposited with the high temperature cap process, see Fig. 3 and 4 above. For the 900°C (Fig. 9D) and 850°C (Fig. 10A) bake temperatures oxide peaks are observed at the growth interface indicating that some oxide remained at the surface prior to epitaxial growth. All films, with the exception of the film represented by the data in Fig. 10B, received no wet cleaning treatment prior to loading in the reactor. Note in Fig. 10B that the oxide peak was significantly reduced by dipping the sample in HF prior to the 850°C bake. This is in contrast to the sample of Fig. 10A which received no HF treatment.

Carbon at the interface was evaluated to a lesser degree. It was noted, however, that one did not detect carbon for bakes above 850°C. Only minor peaks of carbon were observed for the 850°C bakes above the background level of the SIMS tool (2×10^{18}/cm^3).

Film quality.—Characterization techniques addressing film quality included decoration by Yang and Wright etch, as well as MOS measurements. The MOS measurements and etch experiments were performed on films having thicknesses of 1-2 μm. The MOS measurements were made using 1.5 mm aluminum dots over 100 nm oxide films grown on the epitaxial films. Spacing between dots was 0.9 cm center to center. Depletion layer generation cur-

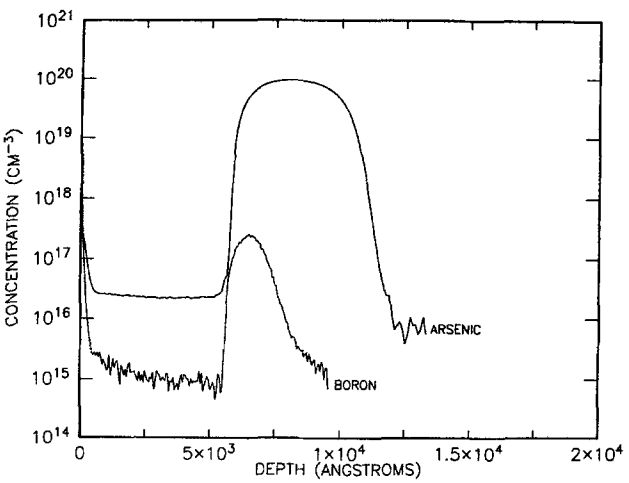

Fig. 6. SIMS dopant profile showing lateral autodoping of boron in an n-type epitaxial film over an arsenic /// n+ region.

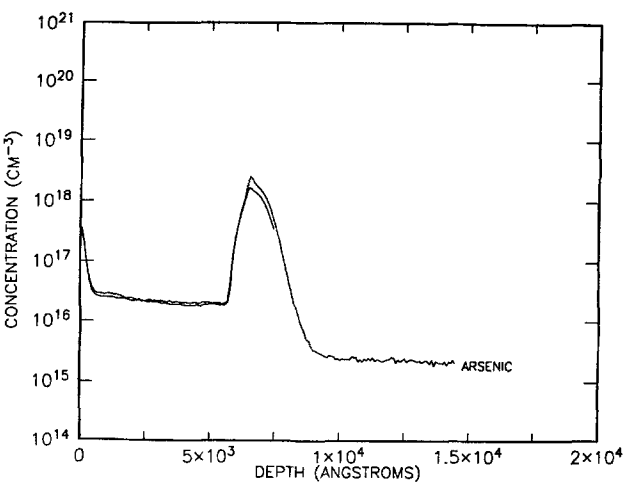

Fig. 8. SIMS profiles showing arsenic concentrations at 30 and 200 μm from an arsenic edge.

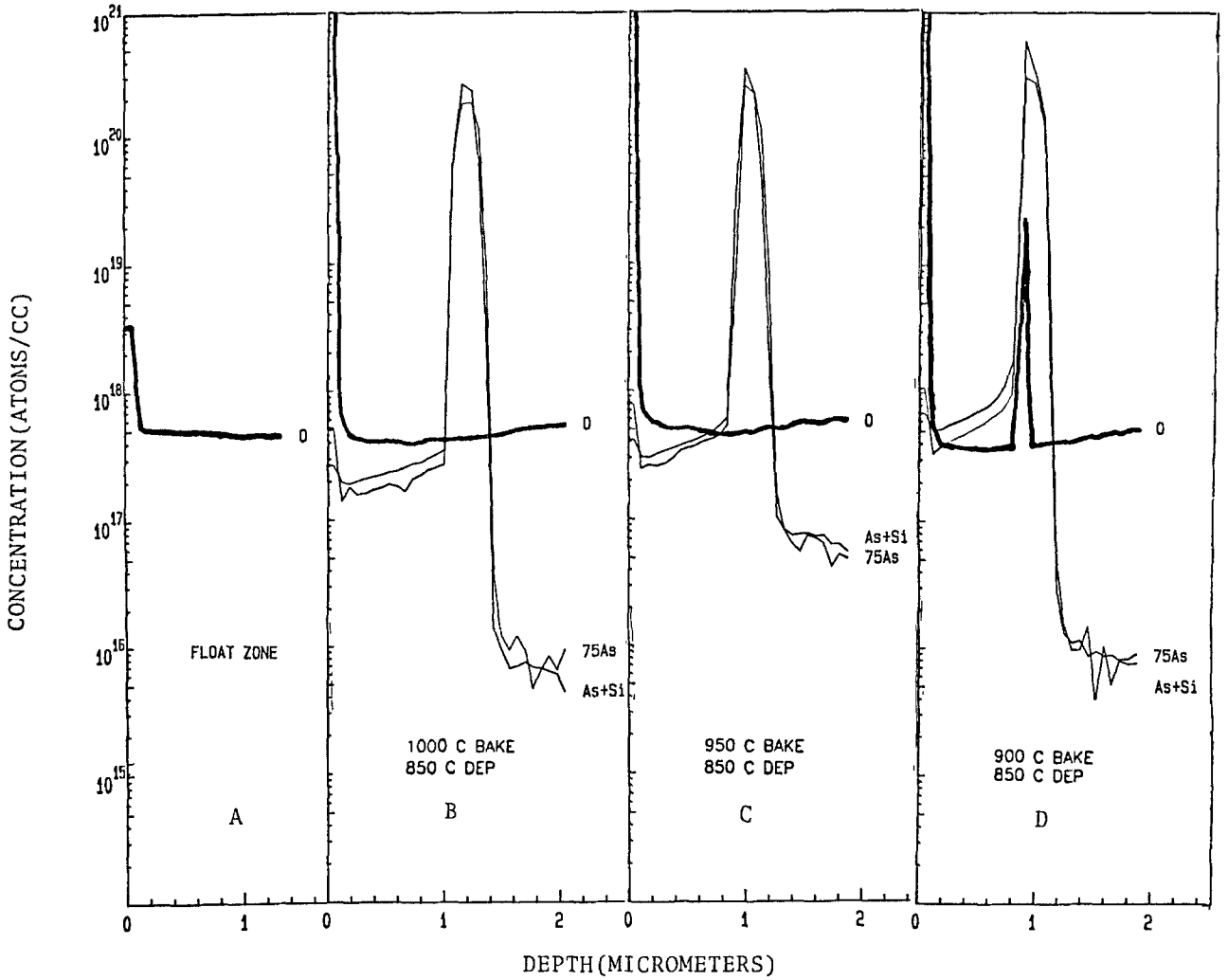

Fig. 9. SIMS profiles showing oxygen levels in MTE films compared to float zone silicon

rents were measured after pulsing silicon into deep depletion to a band bending of 10V. Sampling of 36 dots/measurement gave typical yields of 100% when films were defect-free. Yield is defined as fraction of dots having currents below 500 pA. Good yields correlated with near zero defect count observations using Yang and Wright etch decoration whereas samples with visible counts microscopically gave zero yields. High etch pit counts and low yield correlated with conditions for which the native oxide was not removed as in Fig. 9D and 10A. Surface haze in these samples was easily seen through visual and microscopic examination. Figure 11 shows typical pulsed MOS data for a defect-free film grown at 860°C. Similar results were obtained for films deposited at 850°C (see Fig. 9B, C, and Fig. 10B). Good films were also characterized by a tight distribution for the leakage values as shown in Fig. 11. Films which displayed yield numbers of 50-60% showed a wide distribution of leakage values. TEM results for films in runs showing good retention time yields showed no defects present.

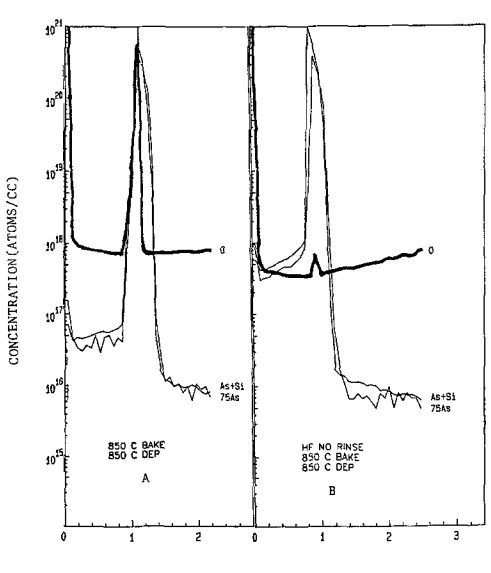

Fig. 10. SIMS profiles for oxygen levels in MTE films grown at 850°C, bake and deposit, with and without HF.

Summary and Conclusions

Device quality films can be deposited in the temperature range of 850°-1000°C. Similar temperatures can be employed in the hydrogen bake to reduce native oxide and carbon prior to film growth. MOS measurements and wet

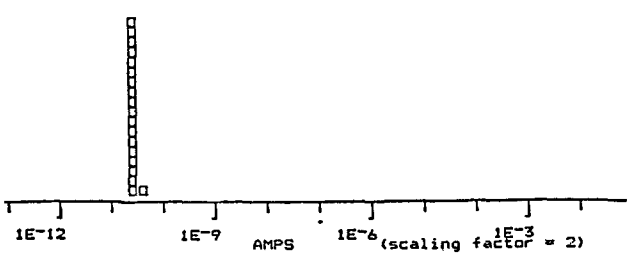

Fig. 11. Histogram of leakage currents for a typical epitaxial film deposited at 860°C. Currents were determined from pulsed MOS measurements on 1.5 mm dots.

etch techniques confirm the MTE film quality obtained. The MTE growth conditions reduce autodoping and produce abrupt doping transitions. Lateral autodoping is observed on n+/p+ surfaces using a two-step cap process. This shows that initial outgassing of both dopants floods the surface at considerable distances from the heavily doped regions. This is particularly severe for the arsenic dopant. For blanket n+ or p+ films, the two-step cap/deposit process reduces autodoping to produce abrupt vertical doping transitions in the films. The MTE film quality is tied to the removal of the native oxide and carbon from the surface prior to film growth.

Acknowledgments

The authors wish to acknowledge Dave Carlson of Applied Materials, for support in the MTE work on the Precision Epi 7700; also D. Schepis and Shaw-Ning Mei of IBM for the later MOS measurements of MTE films deposited in the 7700 tool and Inge Fulton for experimental assistance.

Manuscript submitted June 26, 1989; revised manuscript received Jan. 22, 1990.

IBM General Technology Division assisted in meeting the publication costs of this article.

REFERENCES

1. G. R. Srinivasan, *This Journal*, **126,** 1334 (1980).
2. V. J. Silvestri, G. R. Srinivasan, and B. Ginsberg, *ibid.*, **131,** 877 (1984).
3. B. S. Meyerson, *Appl. Phys. Lett.*, **48,** 12, 797 (1986).
4. T. J. Donahue and R. Reif, *This Journal*, **133,** 1691 (1986).
5. K. H. Yang, in "Semiconductor Processing," ASTM STP 850, Dinesh C. Gupta, Editor, American Society for Testing and Materials, Philadelphia, PA (1984).
6. M. W. Jenkens, *This Journal*, **124,** 757 (1977).
7. E. H. Nicollian and J. R. Brews, "MOS Physics and Technology," pp. 410-412, John Wiley & Sons, Inc., New York (1982).

Phase Relations and the Effects of Ordering in $Zn_{2x}(AgIn)_yMn_{2z}Te_2$ Alloys

Rafael Tovar and Miguel Quintero

Centro de Estudios de Semiconductores, Departamento de Física, Universidad de Los Andes, Mérida, Venezuela

Champa Neal and John C. Woolley

Ottawa-Carleton Institute for Physics, University of Ottawa, Ottawa, Ontario, Canada K1N 6N5

ABSTRACT

The T *vs.* composition phase diagram of the alloy system $Zn_{2x}(AgIn)_yMn_{2z}Te_2$ ($x + y + z = 1$) was investigated in the range $0 < z < 0.7$ by differential thermal analysis and x-ray diffraction measurements. Samples were prepared for various lines of constant x/y ratio and the $T(z)$ data determined for each line. Values of lattice parameters were determined for all samples and the limits of single-phase solid solution estimated. In addition to liquidus and solidus curves, the zinc-blende → chalcopyrite and Mn-disordered → Mn-ordered transition lines were determined, these phase fields being the ones of interest in the measurements of optical energy gap and of magnetic properties.

Most of the work (1, 2) on semimagnetic semiconductor alloys has been concerned with alloys of the form $II_{1-z}Mn_zVI$. However, similar alloys can be produced from the chalcopyrite $I.III.VI_2$ compounds, the ternary analogs of the II VI compounds. The crystallographic and optical energy gap values of a number of alloy systems of the form $(I\ III)_{1-z})Mn_{2z}Te_2$ have been investigated (3-7), and also the work has been extended to the more general $Cd_{2x}(I.III)_{1-z}Mn_{2z}Te_2$ alloys (8, 9).

These chalcopyrite-based alloys are of interest because, depending upon the heat-treatment, the alloys can be produced with the Mn atoms either at random or ordered (or partially ordered) on the cation sublattice. The optical energy gap values and the magnetic behavior are very different in the two different conditions (7-10). Before a detailed investigation of the effects of this ordering can be carried out, it is necessary to choose the heat-treatment of the alloys so as to produce the required ordered or disordered condition. For this purpose, a detailed knowledge of the T *vs.* composition phase diagram is required. Most of the work so far has been concerned with the Cd-base alloys [*e.g.*, (3, 4)], with little work on Zn-based materials. Garbato and Ledda (11) investigated the crystallography of the Zn_{2x} $(CuIn)_{1-x}Te_2$ alloys, and recently the present authors have given the crystallography and optical energy gap values of the $Zn_{2x}(CuIn)_yMn_{2z}Te_2$ and $Zn_{2x}(AgIn)_yMn_{2z}Te_2$ alloys (12). In the present work, this investigation of the Zn-based alloys has been extended to the study of the $T(z)$ diagrams of various sections of the alloy system $Zn_{2x}(AgIn)_yMn_{2z}Te_2$ ($x + y + z = 1$).

Preparation of Samples and Experimental Measurements

All of the alloys used were produced by the usual melt and anneal technique (12, 13). The components of each 1.5g sample were sealed under vacuum in small quartz ampuls, which had previously been carbonized to prevent interaction of the alloy with the quartz, and heated to 1150°C. This temperature is lower than the melting temperature of manganese, which will, however, dissolve in the liquid

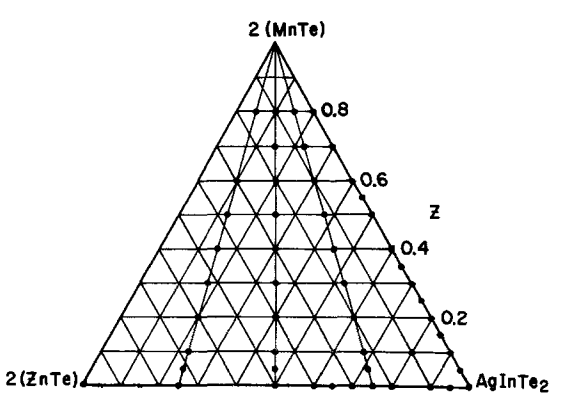

Fig. 1. Composition diagram for the $Zn_{2x}(AgIn)_yMn_{2z}Te_2$ alloys. ● Composition of alloys used in the present work.